



NORSAR Scientific Report No. 1-2011

Semiannual Technical Summary

1 July - 31 December 2010

Frode Ringdal (ed.)

Kjeller, February 2011

6.3 S-Velocities in the crust and uppermost mantle of northern Fennoscandia deduced from dispersion analysis of Rayleigh waves

6.3.1 Introduction

The frequency dependence of phase and group velocity of surface waves can be used to invert for the S velocity in the uppermost layers of the Earth. The classical method for this inversion is the so-called two-station method in which the propagation speed of surface waves is measured between two stations along great circle paths. Measuring this velocity in different frequency bands directly results in a dispersion curve. This dispersion curve can then be inverted for a depth-dependent S-velocity structure between the two stations.

By means of the two-station method a dispersion analysis was carried out in northern Norway. The purpose for these measurements was to investigate the structure of crust and uppermost mantle in this region with special attention to the location of the Mohorovicic discontinuity (Moho). **Fig. 6.3.1** shows a map with the used network of seismic stations. Most of the stations belonged to the temporary network MASI-99, installed for about five month during summer 1999 in Finnmark in a joint project with the University of Potsdam, Germany. The MASI-99 sites were equipped with 13 mobile Lennartz MARSlite data logger and three-component LE-3D/5s seismometers (Schweitzer, 1999). In addition, we analyzed the recordings from a KS-36000 seismometer located at the center site of the ARCES array and from a CMG-3T seismometer installed at the IRIS-station KEV in northernmost Finland. For calibration reasons and to close an operational outage due to upgrade work at ARCES, one of the MASI-99 stations was temporarily co-located with the center site of the ARCES array.

6.3.2 Results with the two-station method

In this study the phase velocity was calculated from the cross-correlation between the vertical seismograms of one event recorded at two stations. Since Love-wave dispersion may have large uncertainties due to interference effects (Knopoff, 1971), we focused in this study on observation and interpretation of the fundamental-mode of Rayleigh waves. Nevertheless, comparison between the 1D-models for the S-wave velocity from the Love wave and the Rayleigh wave dispersion may give in the future interesting results with regard to possible S-velocity anisotropy.

In case of horizontally homogeneous velocities, the phase spectrum of the cross-correlogram does not depend on the epicentral distance of the actual source. Therefore, it is possible to average a number of phase-velocity curves for different events occurring at arbitrary epicentral distances but situated close to the great circle crossing the two stations (Dziewonski and Hales, 1972).

For this study, we selected 24 events with a minimum magnitude of $m_b = 5.5$ in an epicentral distance range from 10° to 120° (see **Table 6.3.1** and **Fig. 6.3.2**). Of all the data to analyze, the recordings from the 5-s seismometers of the MASI stations have the lowest resolution for long period signals. To get a homogeneous data set, the data from ARCES and KEV were converted to simulate a LE-3D/S response; all data were resampled for a common digitalization rate of 1 Hz.

For each event, the 105 possible direct lines between the 15 sites were tested if they follow the propagation direction of Rayleigh waves along a great circle from the source.

However, there were not enough data available to apply the two-station method for each of the 105 station combinations. This was mostly due to the relatively short installation period of the MASI-99 stations and due to the azimuthally uneven seismicity distribution. To solve this problem, also station combinations were analyzed where the direct connection line between the stations does not follow very closely the great circle path. In these cases a too high propagation velocity (*i.e.* an apparent velocity) will be measured. To correct for this effect, all observed phase velocities were multiplied by the cosine of the angle between the great circle direction of the surface propagation and the connection line between the two stations investigated. With this correction data could be analyzed of up to about 30° difference between wave-propagation direction and great circle path through the two stations.

Since this was on the one hand successful, there were on the other hand still too few events available for analyzing single station combination. Therefore, we combined several station combinations to four main directions as shown in **Fig. 6.3.1**, for which average phase velocity curves were calculated. The inversions for the different directions N-S, E-W, and NE-SW lead to similar results for a Moho depth of about 40 km, only on the NW-SE profile we found indications for a slightly deeper Moho. However, these differences were close to the resolution limits of the inversion method, and we decided to invert all data together for a mean S-velocity model below Northern Fennoscandia. **Fig. 6.3.3** shows all 419 measured phase-velocity curves.

On top of **Fig. 6.3.4** the calculated mean dispersion curve of the 419 measured phase-velocity curves (red line) is shown together with its standard deviation (red dashed lines). This dispersion curve was inverted for an 1D S-velocity model. As shown in **Fig. 6.3.3** the mean dispersion curve is reliably determined in a frequency band between 25 and 100 mHz (*i.e.* in a period range between 10 and 40 s). According to Seidl and Müller (1977) the S-wave velocity has the greatest influence on the phase velocity of a Rayleigh wave c_R in a depth of $0.4 \cdot \lambda_R$ where λ_R is the wavelength of the Rayleigh wave. Assuming a mean phase velocity of about 4 km/s in the observed period range the corresponding resolvable depth range is about 15 to 60 km. The lower part of **Fig. 6.3.4** shows the two S-velocity models, the start model for the inversion (black line) and the model best explaining the observed phase velocities (in red) including an uncertainty range (blue). The resulting 1D-model for the S-wave velocities contains a clearly visible Conrad discontinuity. Moreover, the Moho is located slightly above 40 km depth, the sub-Moho S-wave velocity is between 4.6 and 4.7 km/s, and there is some indication for a low velocity channel in the lower lithosphere. As expected from the resolution estimation, the uncertainties become large below 90 km depth.

6.3.3 Comparison of the velocity model with other results

Since the single dispersion curves show a large scatter (see **Fig. 6.3.3**) the calculated mean dispersion curve have to be validated. Therefore, dispersion curves for Rayleigh waves were calculated with another method: the single stations for which the data were analyzed can also be seen as single sites of a large seismic array with a maximum aperture of about 330 km. Then array techniques can be used to measure the mean propagation velocity of the Rayleigh waves.

Eight events were selected (marked with stars in **Fig. 6.3.2** and in **Table 6.3.1**) and bandpass filtered into narrow frequency bands. For each frequency band the phase velocity was measured

with the broadband f-k analysis. Whenever the corresponding backazimuth confirmed the theoretical source direction this observed phase velocity was assigned to the middle frequency of this frequency band. The such determined eight dispersion curves are shown in the upper part of **Fig. 6.3.5**. In the lower part of this figure, one can see that the mean dispersion curve estimated from all f-k results differs from that mean curve calculated from the two-station method but it still lies within the standard deviations. Some of the discrepancies may be explained by the inexact assignment of the f-k measured phase velocities to the frequency band. According to **Fig. 6.3.4** the results from the inversion of the f-k measured phase-velocity curve are shown in **Fig. 6.3.6**. The clearest difference between the two presented 1D-models for the S-wave velocity is the location of the Moho. Where the Moho lies above 40 km depth in the model calculated from the two-station method, the Moho is now deeper than 40 km.

As mentioned above, the MASI-1999 project was a cooperative experiment with the University of Potsdam, Germany. There colleagues deduced S-wave velocity models for crust and uppermost mantle by applying the receiver function method (Jens Höhne and Frank Krüger, private communication). **Fig. 6.3.7** shows on top one 1D-model for the S-velocities estimated with the receiver function analysis. This model also contains a pronounced Conrad discontinuity but in contrary to our results, the Moho now consists of a gradient zone between about 40 and 60 km depth. To check, if this model would also explain the observed phase velocities, the Rayleigh-wave dispersion curve was calculated for this model and plotted together with the above estimated mean dispersion curves (**Fig. 6.3.7**, bottom). The black lines show the mean dispersion curve from the two-station method and its standard deviations, the red line shows the dispersion curve from the f-k method, and the green line shows the dispersion curve calculated from the S-velocity model derived with the receiver-function method. The dispersion curve from the receiver-function method is nearly the same as that one from the f-k method and both lie within the standard deviation of the curve from the two-station method.

6.3.4 Discussion

Although the discussed models differ in several features, they are all in agreement with the observed Rayleigh-wave phase velocities. For all models a two-layer crust is common with a pronounced velocity jump at a Conrad discontinuity in about 15 km depth. The exact depth and structure of the Mohorovicic discontinuity is at the moment an open question because the resolution of the dispersion curves is not good enough to distinguish between a sharp discontinuity at about 40 km depth and a transition zone of about 20 km thickness between crust and uppermost mantle. The phase velocity curve for the receiver-function model in the frequency range between 25 and 60 mHz always lies at the lower bound of the observed dispersion curves. This might be an indication that the S-velocities are too low in the receiver-function model below a depth of about 30 km. A joint modelling of dispersion curves and receiver functions with their different model sensitivity would be needed to solve these discrepancies.

Katja Dietrich, Ruhr-University Bochum
Johannes Schweitzer
Thomas Meier, Ruhr-University Bochum

References

- Dziewonski, A. M. and A. L. Hales (1972): Numerical Analysis of Dispersed Seismic Waves, *Methods in Computational Physics* **11**, Seismology: Surface Waves and Earth Oscillations, Academic Press.
- Knopoff, L. (1972): Observation and inversion of surface wave dispersion, *Tectonophysics* **13**, 497-519.
- Schweitzer, J. (1999): The MASI-1999 field experiment. NORSAR Semiannual Tech. Summ. 1 April - 30 September 1999, NORSAR Sci. Rep. No. **1-1999/2000**, Kjeller, Norway, 91-101.
- Seidl, D. and S. Müller (1977): Seismische Oberflächenwellen, *J. Geophys.* **42**, 283-328.

Table 6.3.1. The table shows the event coordinates used for the two-station method. Events marked with a star were also chosen for the f-k method.

No.	Date	Time	Lat	Lon	Depth	mb	ms	
	year.doy	[hr.min.sec]	[°]	[°]	[km]			
1	1999.169	10.55.25.80	5.510	126.640	33.0	6.1	6.1	
2	1999.180	23.18.05.60	36.620	71.350	189.3	5.9	0.0	
3	1999.182	02.06.58.40	70.390	-15.150	10.0	4.9	5.6	*
4	1999.183	11.45.31.30	49.370	-129.200	10.0	5.4	5.7	
5	1999.184	01.43.54.00	47.080	-123.460	40.6	5.4	5.5	
6	1999.188	18.52.57.00	49.230	155.560	33.0	6.0	5.6	
7	1999.193	03.42.17.00	30.070	69.420	51.5	5.4	5.6	
8	1999.218	00.32.41.70	49.930	156.260	57.8	5.5	5.5	
9	1999.225	13.05.54.50	43.810	149.140	43.0	5.6	5.2	
10	1999.226	00.16.52.30	-5.890	104.710	101.4	6.0	5.7	
11	1999.229	00.01.39.10	40.750	29.860	17.0	6.3	7.8	*
12	1999.238	01.24.42.60	10.380	126.010	62.6	5.6	0.0	
13	1999.238	07.39.28.90	-3.520	145.660	33.0	5.6	6.2	
14	1999.238	21.38.11.90	19.120	121.150	33.0	5.5	5.2	
15	1999.241	00.46.13.50	3.100	65.860	10.0	5.8	5.6	
16	1999.250	11.56.49.40	38.120	23.600	10.0	5.6	5.8	*
17	1999.256	11.55.28.20	40.710	30.050	13.0	5.8	5.8	*
18	1999.258	03.01.24.30	-20.930	-67.280	218.0	6.0	0.0	
19	1999.263	09.32.42.70	46.330	153.460	33.0	5.6	5.1	
20	1999.263	17.47.18.50	23.770	120.980	33.0	6.5	7.7	*
21	1999.263	21.46.42.90	23.390	120.960	33.0	5.8	6.5	*
22	1999.265	00.14.39.20	23.730	121.170	26.0	6.2	6.4	*
23	1999.268	23.52.48.70	23.740	121.160	17.0	6.2	6.4	*
24	1999.271	05.00.43.00	54.590	168.260	33.0	5.4	6.1	

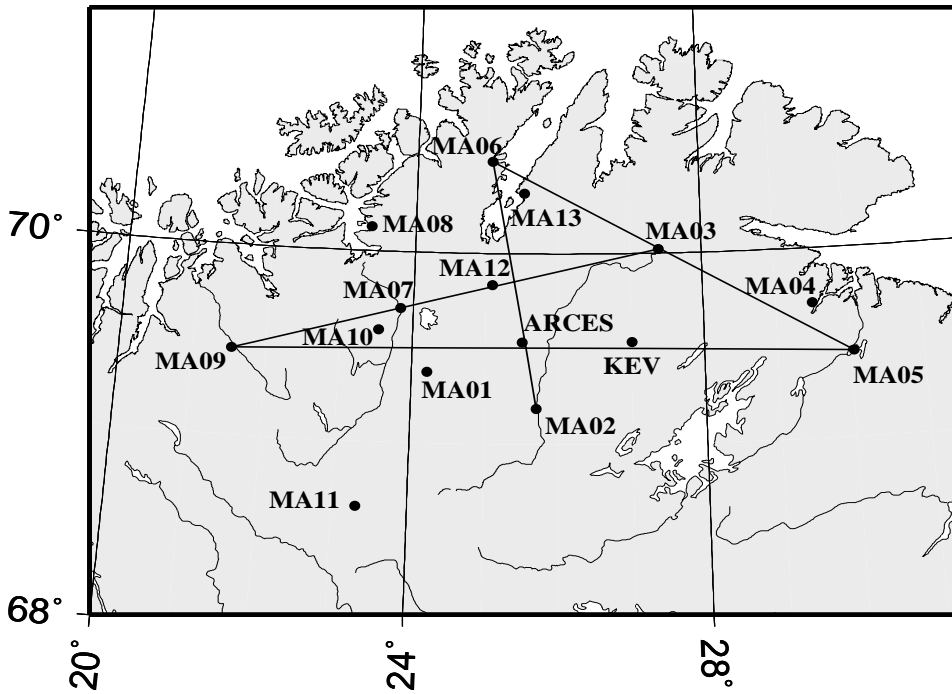


Fig. 6.3.1. Map of all seismic stations used in this study: the 13 stations of the temporary network MASI-1999 and the permanently installed ARCES array and IRIS-station KEV. The MASI-1999 station MA00 was temporarily co-located with ARCES array site ARA0. The four lines show the main profiles along which subsets of the data were interpreted.



Fig. 6.3.2. A map showing the epicenters of all events used for this study. According to Table 6.3.1, data from events marked with a star were also analyzed with the f-k method.

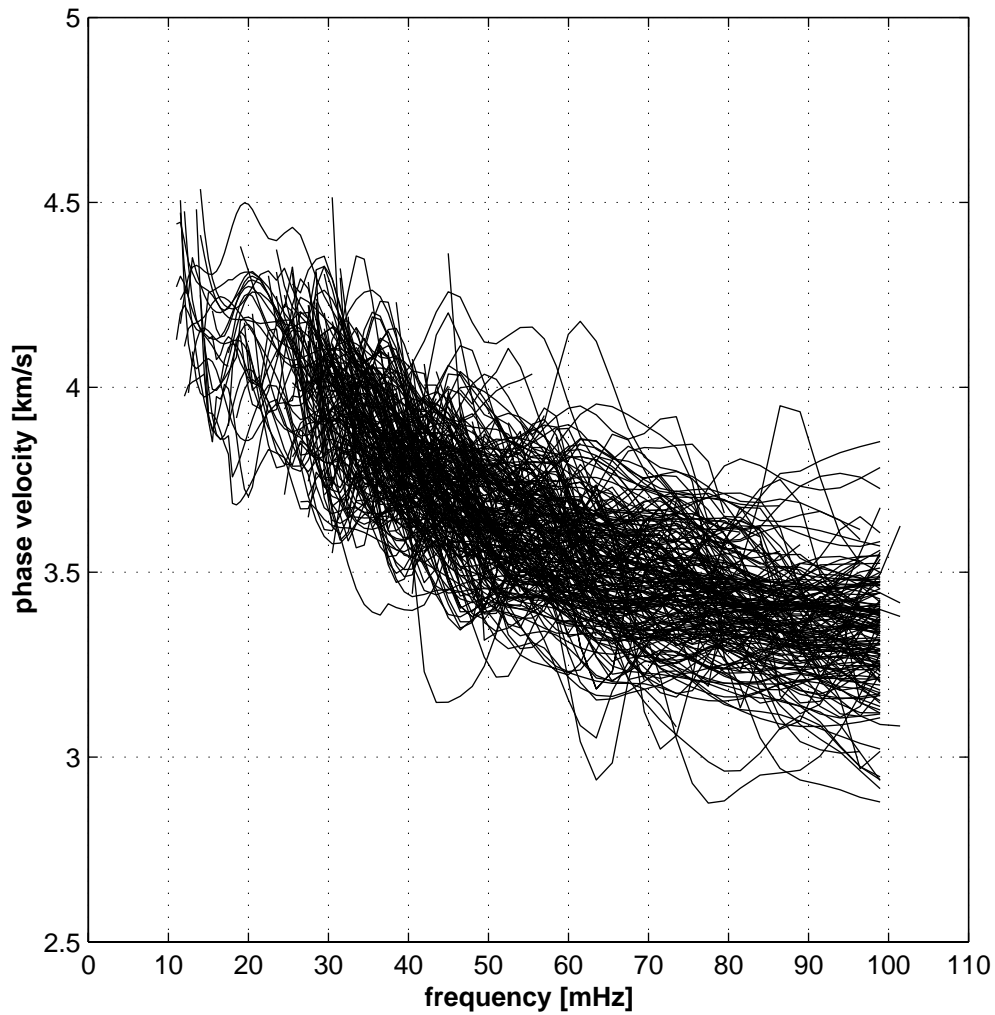


Fig. 6.3.3. All 419 dispersion curves of Rayleigh-wave phase velocities in Northern Fennoscandia determined in this study with the two-station method between. A sufficient amount of observations to invert for the S-velocity structure is available in the frequency range between 25 and 100 mHz (i.e. periods between 10 and 40 s).

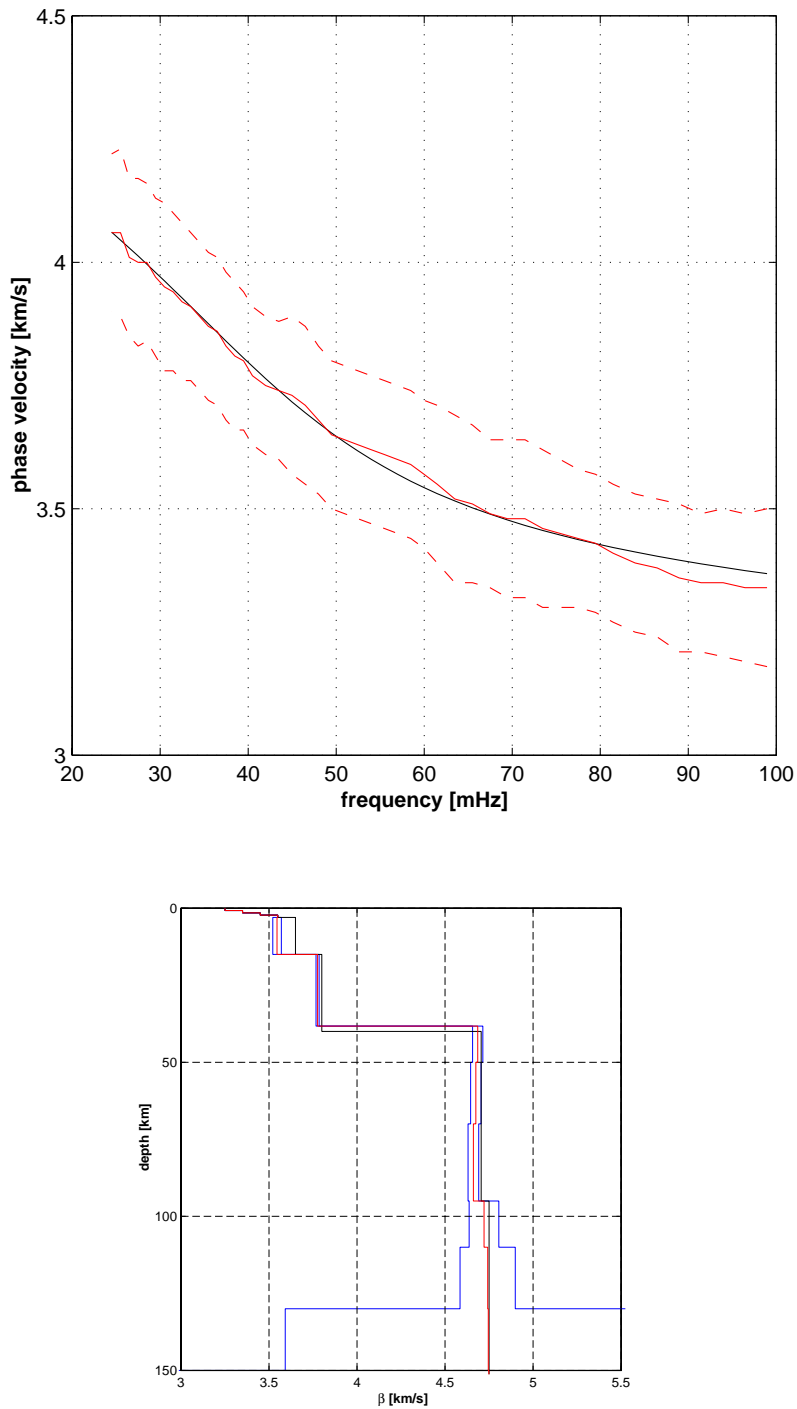


Fig. 6.3.4. On top one can see the resulting mean dispersion curve together with its standard deviations as a red line and red dashed lines, respectively. The additional black line is the fitted phase-velocity curve calculated from the resulting 1D-model for the S-wave velocity plotted at the bottom panel (red line). This also includes the reference model used for the inversion (black line) and the standard deviations (blue lines) for the calculated model.

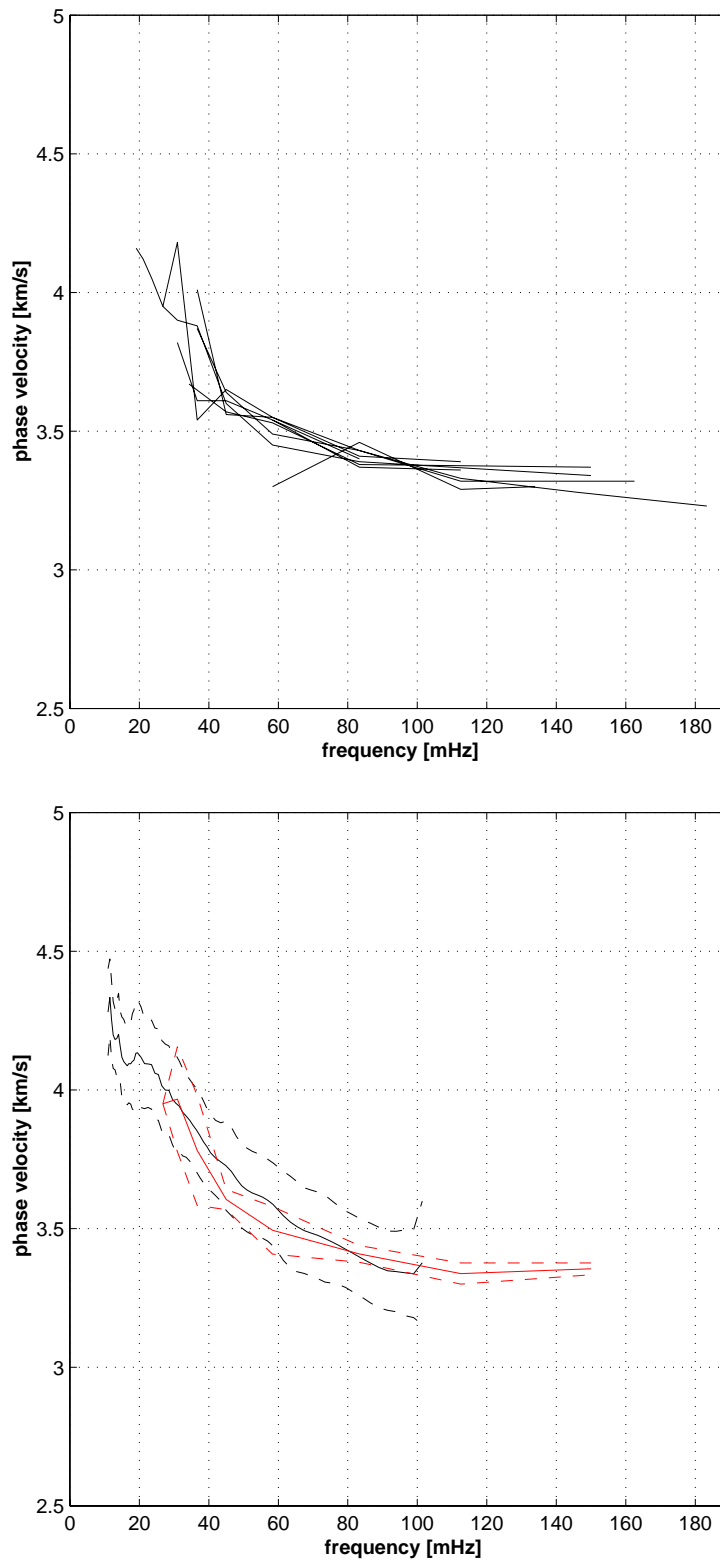


Fig. 6.3.5. The upper part of the figure shows the eight dispersion curves of Rayleigh-wave phase velocities measured by the f-k analysis. The lower part shows a comparison between the mean dispersion curves calculated from the two-station method (black) and from the f-k method (red).

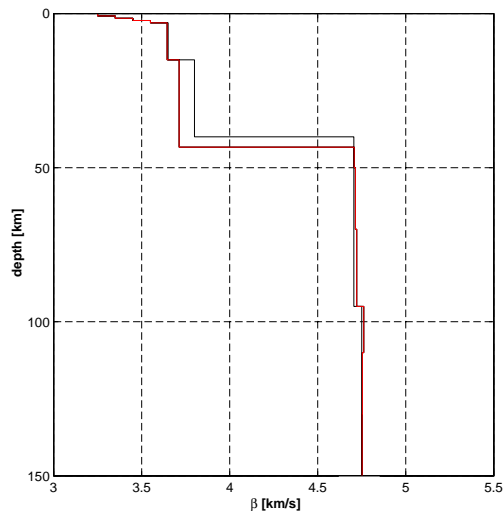
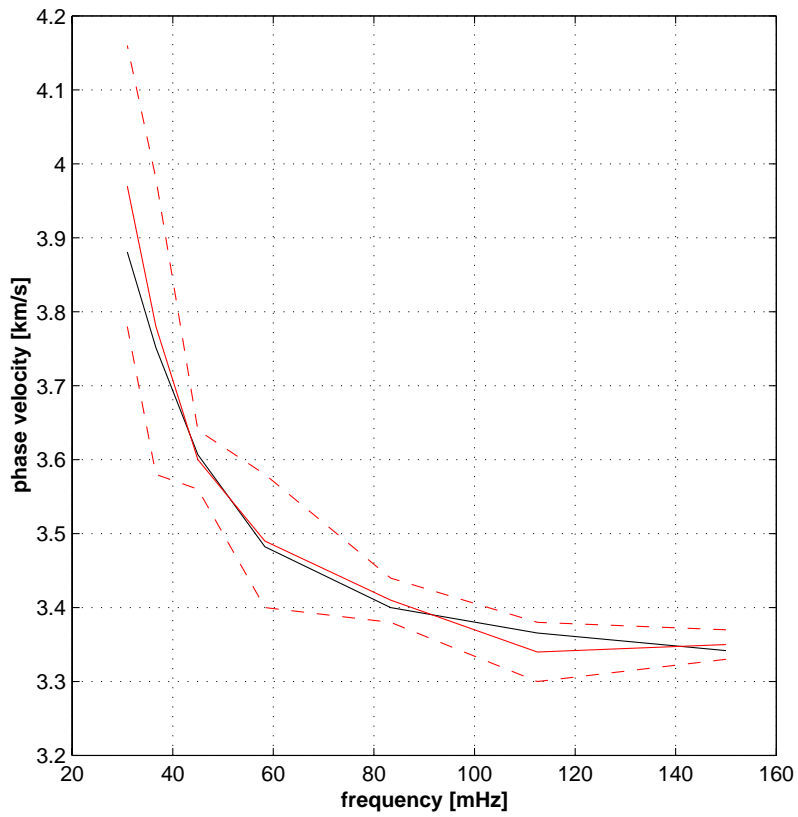


Fig. 6.3.6. The figure shows the results of the dispersion-curve inversion as in Fig. 6.3.4 but with the mean curve resulting from the f-k analysis used as input for the inversion. The main difference in the estimated model is the Moho depth, which is now below 40 km.

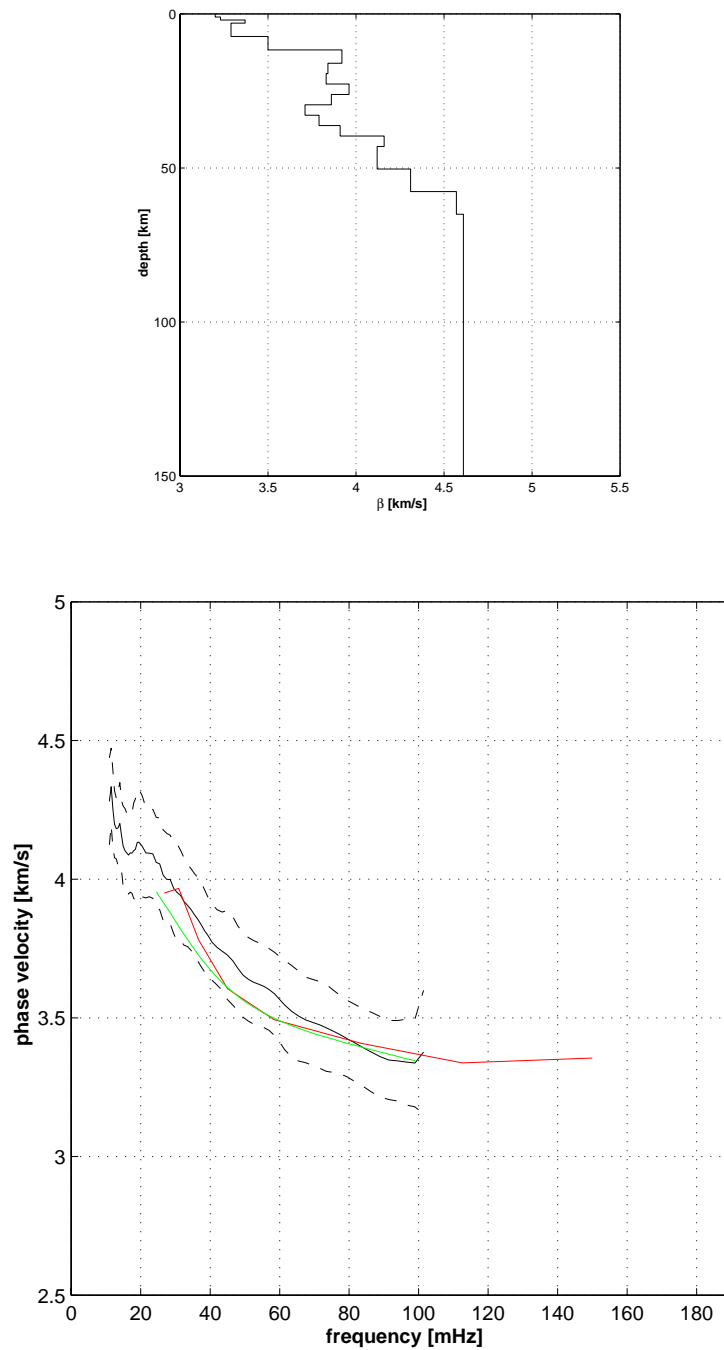


Fig. 6.3.7. The upper panel shows the 1D-model for the S-wave velocity from one of the receiver-function inversions. The lower panel shows a comparison of different dispersion curves: the mean dispersion curve from the two-station method and its standard deviations (black), the mean dispersion curve from the f-k method (red), and the dispersion curve calculated from the S-velocity model estimated from the receiver function.